Proceedings of the 17th Hypervelocity Impact Symposium
HVIS2024
September 9-13, 2024, Tsukuba, Japan

HVIS2024-HV240077

FAILURE MODES OF CFRP PANELS UNDER HYPERVELOCITY IMPACT: THE EFFECTS OF STRAIN RATE BETWEEN 1 KM/S AND 6 KM/S

Jacob Lawrence[1,*], Dr. Jonathan Painter[1], Dr. Alexandra Iordachescu[1,2], Dr. Charles J Footer[1,3], Ryan M Seabright[3], Professor Gareth Appleby-Thomas[1],

[1] Centre for Defence Engineering, Cranfield University, Defence Academy of the United Kingdom, Shrivenham, SN6 8LA, UK
[2] University of Birmingham, Birmingham, UK
[3]QuinetiQ, Farnborough, UK

ABSTRACT

Studying the effects of hypervelocity impacts on structural materials is essential for the aerospace and defense fields. However, there is a paucity of open-source and accessible data in the literature concerning the hypervelocity impact response of CFRP composites. This paper details our results from an experimental research program designed to aid in addressing this limitation by providing extensive data from multiple analysis techniques. This is part of a wider body of research focused on identifying failure modes and their evolution at elevated strain rates. Experimental work on the impact of commercially available CFRP composites at impact velocities between 1000 and 6000 m/s is presented and discussed. This work provides further validation for the response of an aerospace-relevant material to extreme loading conditions, with wider implications for the design and use of these structures in various industries. Preliminary results from optical imaging, HSV capture, SEM, VP-SEM, and target mass loss analysis are included and show a strain rate dependence in the CFRP material studied.

Keywords: CFRP, Hypervelocity impact, Failure modes, Damage evolution

NOMENCLATURE

CFRP	Carbon Fiber Reinforced Polymer
HVI	Hypervelocity impact
HSV	High-speed Video
LGG	Light gas gun
SEM	Scanning Electron Microscopy
VP-SEM	Variable Pressure SEM
fps	Frames Per Second
Px	Pixels

1. INTRODUCTION

The material response of CFRP composites to mechanical stress and impacts involves complex dynamics and interactions between the reinforcing fibers and the polymer matrix. Many experimental and design parameters influence the impacted target's response, including the constituent phases' material properties, the composite's layup or stacking sequence, projectile geometry, material, and impact velocity. For a detailed review of the parameters that influence the impact response of fiber-reinforced composites, please see[1]. Strain rate is also an important contributing factor during impact loading of these materials. Reinforcing fibers, matrix material, and the resulting composite exhibit material behavior sensitive to strain rate; this includes strain rate softening, strain rate hardening, and visco-plastic behavior. [2–6].

Many studies have been undertaken into the impact response of CFRP composites across various velocity regimes and strain rates. These range from low-velocity impacts [7–11] typically encompassing velocities ranging from 0-50 m/s to high-velocity impact regimes ranging from 50-1000 m/s [4,12–17]. However, there is a paucity of experimental data concerning impacts in the hypervelocity regime, where impact velocities can reach several km/s.

This velocity regime is particularly relevant to the space, aviation, and defense sectors, where CFRP composites are increasingly employed due to their high specific mechanical properties and desirable material properties such as corrosion resistance, providing opportunities for weight reduction and increased performance [18]. Several studies have been carried out on the hypervelocity impact response of CFRP composites, including investigations of the shock response of this material class and numerical modeling of hypervelocity impact events. [19–22] Fewer experimental studies have been carried out on the

* Corresponding author: Jacob.lawrence@cranfield.ac.uk

Published by ASME. Issued with: Creative Commons Attribution License (CC:BY 4.0).
Please refer to any applicable publisher terms of use.

hypervelocity impact performance of CFRP composites. Work conducted by Francesconi and colleagues [23] exposed CFRP targets of varying thicknesses to a series of 45 shots, which provided further information on the impact response, failure mechanics, and ballistic limits of CFRP composites in the hypervelocity regime. The research program discussed in this paper is designed to build and improve on the available experimental data, providing open-source results for model validation and verification. It is also being used to interrogate the strain rate sensitivity of this class of composite materials.

Although the definition of the hypervelocity regime is variable depending on the industry or research area, some authors arguing velocities of 1000 m/s constitute a hypervelocity impact [21] and other sources suggesting that hypervelocity impacts occur only when the speed of sound in the material is exceeded [24]. However, it is generally agreed that this velocity regime begins with the onset of hydrodynamic behavior. For CFRP composites, defining this transition is a complicated task due to the complex composition of the material and its various constituent phases. Due to the multi-material nature of these structures, there are several failure mechanisms presented by CFRP composites, which can be attributed to failure modes specific to the matrix and fibers, as well as complex interactions between these phases during mechanical loading, each of which has a subset of characteristic failure mechanisms. Understanding the material behavior and individual responses of these elements across varying strain rates is a challenging task.

This research program takes a holistic approach to identifying the evolution of failure modes displayed by a commercially available CFRP composite panel subjected to impacts over a velocity range of 1-5.5+ km/s. Impact velocities have been selected to span the transition from high to hypervelocity to identify strain rate effects in the material response of our panels to dynamic impact loading in this velocity regime. Further testing of a wider range of CFRP composites over the course of the program is planned to provide a comparison. This will facilitate the interrogation of the failure mechanics of CFRP composites as a class of materials, enabling engineers to more confidently model and predict their behavior, paving the way for the development of novel impact-resistant CFRP composites in applications where hypervelocity impact risks pose a significant threat to operational platforms.

2. MATERIALS AND METHODS

This experimental program employed two variations of commercial CFRP composite plates as targets. These targets were sectioned from larger sheets of the material sourced from Easy Composites Ltd (UK) [25] and consisted of rectangular samples 150mm x 100mm. The target thicknesses employed in this study were nominally 1 and 3 mm. Targets were manufactured using a QI layup, with the following stacking sequences: $[Twill_{210}/\pm45\circ Biax_{300}/Twill_{210}]$, $[Twill_{210}/\pm45\circ Biax_{300}/Twill_{650}/Twill_{210}/Twill_{650}/\pm45\circ Biax_{300}/Twill_{210}]$ for the 1 and 3mm sheets respectively[26].

The projectile material selected for this project was an Al 99% 1000 series aluminum alloy. Aluminum projectiles were chosen due to their relevance in size, weight, and composition to man-made space debris to support the operational context considered. The projectiles used were spheres with nominal diameters of 3 and 4mm. The average mass of the projectiles was $(3.780\pm0.000005)\times10^{-2}$g and $(8.725\pm0.000005)\times10^{-2}$g respectively.

A bespoke clamping system comprising up- and down-range witness plate holders and a target clamp was designed and manufactured for the experiments. This clamping system maintained a repeatable distance of 100mm between witness plates and targets held in a parallel configuration perpendicular to the projectile's flight path. It incorporates a modular design to allow for easy and precise modification of parameters within a short timeframe.

Copper sheets of 3mm thickness were employed for the witness plates. This material was chosen to provide contrast to the aluminum and carbon fiber that would be captured on them to facilitate analysis using SEM.

A 2-stage convertible powder light gas gun was employed to accelerate the projectiles into the targets. The 2-stage LGG was used with a rifled 5.56-mm bore launch-tube and a 7.68-mm smooth bore launch-tube to accelerate the aluminum projectiles at velocities ranging from ca. 1-5.5 km/s using a four-piece split sabot. The 2-stage LGG was equipped with a laser gate velocity measurements system consisting of two sequential gates separated by 300mm connected to a timer to allow for the calculation of impact velocity.

During the experimental campaign, several HSV cameras were employed to capture footage of the impact event. A Phantom V1212 (Vision Research Ltd. – UK) [27] was the primary camera used during all experiments. This was operated at a frame rate of 160,000 frames-per-second (fps). A series of 6 shots were executed that employed a Phantom TMX 7510 camera operating at a frame rate of 860,000 fps and a Phantom T3610 operating at a framerate of 300,000 fps alongside the Phantom V1212 camera to capture multiple angles of the impact events. This data was used qualitatively to capture the contact and impact events across a range of velocities. Quantitative measurements were also taken from the footage to identify the initial impact velocity and the residual velocity of the projectile after impact.

Post-impact analysis was carried out on the targets, which consisted of optical imaging and VP-SEM analysis of the impact sites. Optical imaging was combined with the open-source image analysis software Image J (FIJI) [28] to extract morphometric data on damaged sites. The VP-SEM was used to analyze the fiber fractures around the impact site.

Post-impact analysis of the witness plates employed SEM and optical imaging. The optical imaging was used in conjunction with Image J (FIJI)[28] to identify the evolution of the debris pattern generated on the witness plates. SEM imaging was used to determine the structure and nature of fractures on the residual fibers found on the witness plates, crater morphology, and residual projectile material.

Target plate weights were recorded prior to and post-impact to enable us to record the mass lost in the target during the impact events and to reveal any trends in the amount of material excavated from the targets during perforation.

By combining optical and quantitative results from the HSV capture and forensic post-impact analysis techniques, an understanding of the dynamic behavior of the CFRP composite during the impact can be extracted, providing insight into the evolution of failure modes and the effects of impact velocity and strain rate on the damage evolution in the target and projectile.

Unique Shot I.D.	D_p (mm)	T_t (mm)	V_i (m/s)	Experimental Notes
C0S04	3	3	2180	Successful
C0S05	3	3	1517	Successful
C0S06	3	3	1289	Successful
C0S07	4	1	1953	Sabot impact
C0S08	4	3	1946	Successful
C0S09	4	3	1443	Successful
C0S10	4	3	1000	Successful
C0S11	4	1	1285	Sabot impact
C0S12	4	1	1040	Sabot impact
C0S13	3	1	1200	Successful
C0S14	3	1	1521	Successful
C0S15	3	1	2135	Successful
C1S01	3	1	2403	Successful
C1S02	3	1	4143	Successful
C1S03	3	1	5535	Successful
C1S04	3	3	2870	Successful
C1S05	3	3	4184	Successful
C1S06	3	3	5681	Successful
C1S07	4	1	3452	Successful
C1S08	4	1	4021	Successful
C1S09	4	1	5025	Successful
C1S10	4	3	3554	Successful
C1S11	4	3	3960	Successful
C1S12	4	3	5291	Successful
C1S16	3	3	1312	Successful
C1S17	3	3	1504	Successful
C1S18	3	3	2188	Successful

TABLE 1: SHOT PROGRAM RECORD DETAILING UNIQUE SHOT I.D, PROJECTILE DIAMETER (D_p), TARGET THICKNESS (T_t), IMPACT VELOCITY (V_i) AND EXPERIMENTAL NOTES.

Table 1 describes the experimental campaign undertaken to date and displays information on the target thickness, projectile diameter, and achieved impact velocities.

3. RESULTS AND DISCUSSION

Our results were used to analyze and identify trends in the evolution of failure modes over the velocity regime from ca. 1-5.5 km/s and ascertain information on the strain rate behavior of the material while highlighting areas where further research is needed.

3.1 Optical Imaging.

Photographic records of the targets and witness plates from the experimental campaigns have been acquired and processed to analyze the evolution of perforation holes and witness plate damage patterns. These are presented in Figures 1-4 below.

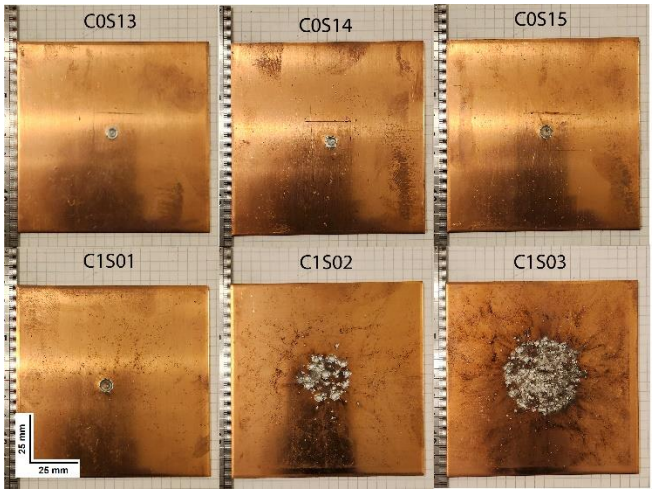


FIGURE 1: WITNESS PLATE RESULTS FROM EXPERIMENTS INVOLVING 3mm Al. PROJECTILE AND 1mm CFRP TARGET AT IMPACT VELOCITIES CA. 1-5.5 km/s.

Figure 1 presents the witness plate impacts following a 3mm Al projectile accelerated into a 1-mm thick CFRP target. There is a clear evolution as impact velocity is increased with a transition from a single crater to a radial damage pattern between the velocities of 2400 and 4143 m/s, indicating a change in failure modes presented by the target and projectile and a dependency on strain rate in this velocity regime. Additional experimentation is required to identify if this is a gradual or discrete change in failure mechanics and to ascertain the velocity at which this occurs. Interestingly, the expected sound speed of the CFRP target Ca. 2.5-3 km/s lies within this velocity range, indicating that shockwave propagation strongly influences the failure modes presented by this material. Further investigation around the sound speed velocity will be undertaken to gain insight into how this affects the damage evolution in the debris cloud.

Figure 2 presents witness plates from impacts of a 3mm projectile into a 3mm target. The transition from single impact crater to multiple impact craters is apparent between 2188 and 2870 m/s and becomes more pronounced with velocities over 4184 m/s. The damage presented at higher velocities differs from the circular pattern witnessed in Figures 2 and 4, suggesting a relationship between target thickness and projectile diameter, which influences the failure of the projectile and target. This relationship has been previously studied at lower velocities by Cao and colleagues [9]. Understanding how this relationship

evolves as impact velocities increase will help unravel the interactions between projectile diameter/target thickness and separate them from strain rate effects.

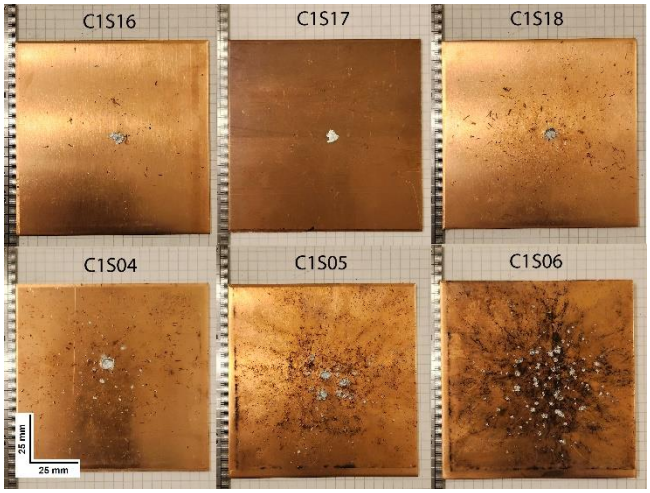


FIGURE 2: WITNESS PLATE RESULTS FROM EXPERIMENTS INVOLVING 3mm Al. PROJECTILE AND 3mm CFRP TARGET AT IMPACT VELOCITIES CA.1-5.5 km/s.

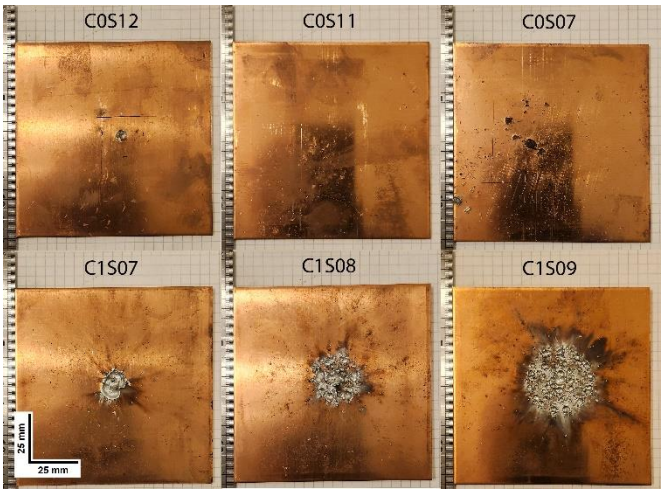


FIGURE 3: WITNESS PLATE RESULTS FROM EXPERIMENTS INVOLVING 4mm PROJECTILE AND 1mm TARGET AT IMPACT VELOCITIES CA.1-5.5 km/s.

Figure 3 presents the witness plates from impacts of a 4mm projectile into a 1mm target and shows a similar evolution in damage pattern to that in Figure 2. Shots C0S11 and C0S07 were not completely successful, as secondary impacts also occurred on the targets from the sabot used to house the projectile. These were due to insufficient separation of the segments during the launch process, which can sometimes occur. Therefore, the transition between damage patterns is more difficult to assess. The higher velocity shots display the same evolution of the damage pattern seen in Figure 1. It is interesting to note that the projectile diameter is much greater than the target thickness in both of these situations and leads to a similar evolution in damage patterns, suggesting that when the projectile is overmatched to the target, there is a specific set of damage mechanisms that occur and that the evolution of these damage patterns is primarily driven by impact velocity, shock wave behavior, and strain rate effects.

Figure 4 presents the witness plates from impacts of a 4-mm diam. sphere into a 3-mm thick target and shows an evolution of damage patterns similar to those in Figure 2, with the transition from a single impact crater to multiple craters becoming evident between velocities of 1946 and 3554 m/s, this evolution continues as impact velocities increase with the spread of the damage area increasing.

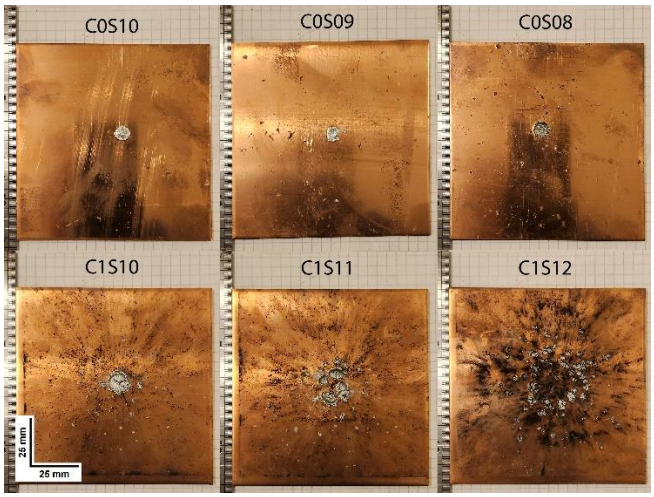


FIGURE 4: WITNESS PLATE RESULTS FROM EXPERIMENTS INVOLVING 4mm PROJECTILE AND 3mm TARGET AT IMPACT VELOCITIES CA.1-5.5 km/s.

To summarize, the witness plates show two distinct damage patterns linked to target thickness, with Figures 1 and 3, 1-mm target thickness, presenting similar evolutions in witness plate damage as strain rates increase. Figures 2 and 4 again show a strong resemblance in the evolution of damage patterns with increasing impact velocities. This provides strong evidence for different failure mechanisms dependent on the target thickness and projectile diameter. The evolution of crater morphology on the witness plates as impact velocities increase shows clear evidence of an evolution of failure modes dependent on strain rate.

The differences in the damage patterns of the witness plates can be attributed to a range of factors, including the relationship between target thickness and projectile diameter, the onset of hydrodynamic behavior where material strength no longer plays a role in the evolution of damage in the target or projectile and the shock response of the materials dominates, the onset of strain rate effects, changes in thermomechanical localized heating, or the onset of impact flash emissions and phase transitions in the target and projectile materials. To fully understand how the damage mechanics and the dynamic response of the target materials evolve, it is essential to consider the interplay between these factors and try to isolate individual effects.

3.2 Target Mass Loss

Figures 5 and 6 illustrate the resultant mass loss from the target at various impact velocities for each target and projectile pairing. The plot ranges are provided on a conformal scale of 0 to 6000 m/s for velocity, from 0 to 0.2 g (1mm targets), and from 0 to 0.6 g (3mm targets) for mass lost to facilitate comparisons.

Figure 5 shows that the 1mm thick targets exhibit a plateau in mass loss past a velocity threshold of between 2000 m/s and 2500 m/s. This contrasts with the general trend of increasing mass loss with increasing velocity for the 3mm targets shown in Figure 6, which follows a near-linear relationship as impact velocity increases.

For the 1mm targets, there is contrasting behavior depending on projectile size; the 3mm projectiles show little difference in mass loss across the entire velocity regime, whereas the 4mm projectile impacts show an increase in the mass loss in the velocity range of 1000-2000 m/s followed by an asymptotic response at higher velocities. This provides further evidence to reinforce the relationship between projectile diameter and target thickness seen in witness plate data.

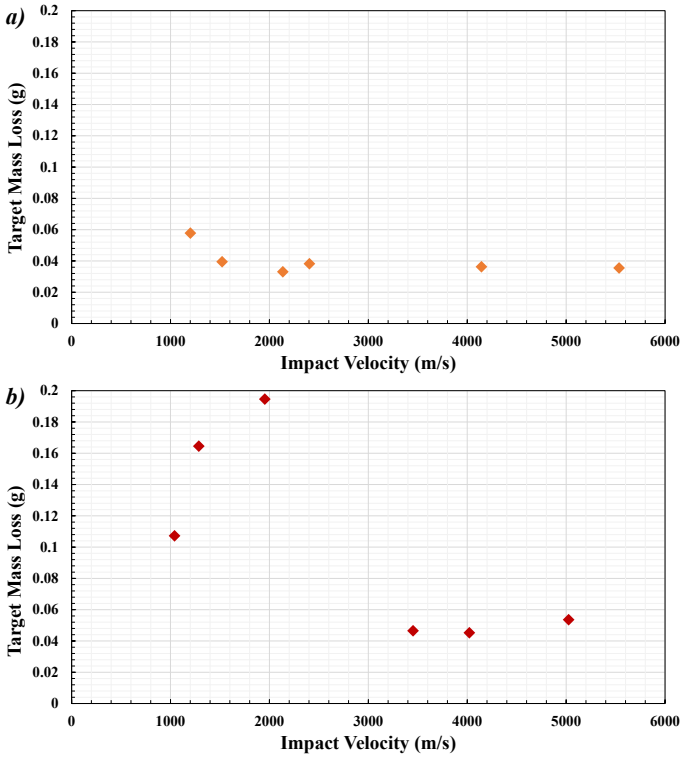


FIGURE 5: VELOCITY VS. MASS LOSS PLOTS FOR 1mm CFRP TARGETS IMPACTED BY a) 3mm DIA. b) 4mm DIA. AL SPHERES.

Figure 6 shows that for the 3-mm thick targets, there is a distinct trend for both projectile sizes where there seems to be a direct relationship between impact velocity/strain rate and mass loss in the target. This relationship appears linear in both the 3mm target 3mm projectile pairing and except for the 1000 m/s impact in the 3mm target 4mm projectile pairing.

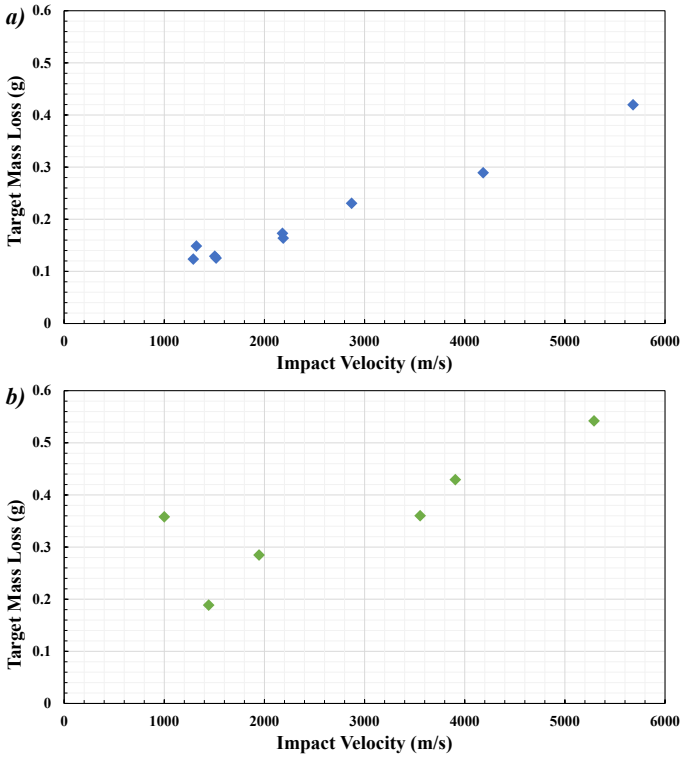


FIGURE 6: VELOCITY VS. MASS LOSS PLOTS FOR 3mm CFRP TARGETS IMPACTED BY a) 3mm DIA. b) 4mm DIA. AL SPHERES.

Based on these results, we can conclude that there appears to be a threshold where impact velocity/strain rate influences the behavior of overmatched target projectile pairings. This transition appears to occur between the velocities of 2 and 3 km/s. Further impact experiments will be executed in this velocity range to interrogate the mechanisms behind this and identify whether this is a smooth transition or if the transition happens abruptly. The change in behavior in this velocity regime may be linked to the sound speed of the material, shock response, strain rate effects, or inertial effects and requires further investigation through the addition of more data points across this velocity range to be fully understood.

For the 3-mm thick targets, this relationship does not appear to be present, indicating that different failure mechanisms are responsible for the excavation of mass during the impact event and that the relationship between projectile diameter and target thickness plays a crucial role in the underlying physical processes of damage evolution.

3.3 High-Speed Video Analysis.

A catalog of HSV videos of impacts on CFRP targets was compiled to provide an open-source resource for model validation and to investigate impact dynamics.

Figure 7 shows frames captured from a Phantom TMX 7510 at a resolution of 640 x 128 px with a frame rate of 860,000fps. The images show a distinct change in the morphology of the

down-range ejecta between impact velocities of 2188 and 2870 m/s. For the impact velocity of 2188 m/s and below, the projectile remains relatively intact, with larger flakes of the CFRP target present in the debris generated. Once the impact velocity increases to 2870 m/s, the projectile has been at least partially fragmented during the impact event, and the debris cloud consists of much finer particulate matter, which forms a conical debris cloud with a spherical leading edge; this is in contrast to the lower impact velocities where this morphology is not present. As impact velocity is increased further, the debris cloud becomes more dense and the conical shape of the debris cloud becomes more pronounced.

This transition between intact and fragmented projectiles occurs in the velocity range where we expect to find the sound speed of the CFRP target (circa velocity of 2.5-3 km/s). This indicates that once the impact velocity exceeds the sound speed of the target, failure becomes dominated by shock response, and there is a distinct change in failure mechanisms as impact velocity and strain rate increase.

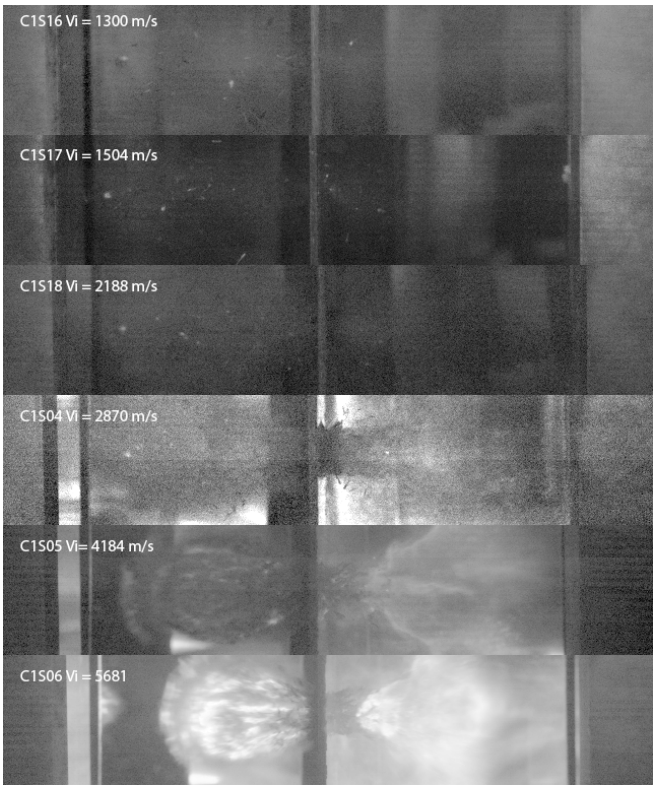


FIGURE 7: HSV FRAMES FROM 3MM DIAMETER Al SPHERE INTO 3MM CFRP TARGET, CAPTURED WITH A PHANTOM TMX 7510 AT 860,000 fps.

Using the built-in capabilities of the phantom camera control software PCC (Vision Research Ltd – UK) [29], measurements of the projectile's velocity were taken before and after impact. In the case where the projectile was still intact, the residual velocity measured was of the projectile itself, and in the case where there was fragmentation and the formation of a debris cloud, the velocity of the leading edge of the debris cloud was taken. The change in velocity was then plotted against the initial impact velocity, as shown in Figure 8. It can be seen from this plot that there is a near-linear relationship between initial impact velocity and residual velocity, irrespective of projectile damage.

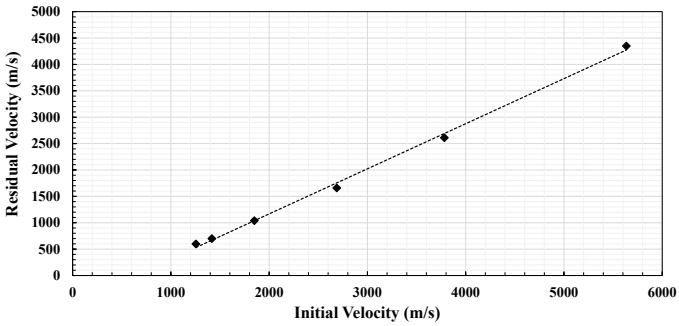


FIGURE 8: PLOT OF INITIAL VELOCITY VS RESIDUAL VELOCITY CALCULATED FROM HSV FOOTAGE OF SHOTS C1S04, 05, 06, 16, 17, 18.

3.4 SEM and VP-SEM analysis.

Witness plates from the impact experiments were analyzed at high resolution using scanning electron microscopy to interrogate surface and topographical features following damage. Target plates were interrogated using VP_SEM to prevent the charging of the CFRP targets.

Images from the central impact site and surrounding areas were taken at both low (10X) and high (420X) magnifications for the witness plates. Figure 9 below shows 10X magnification images of the impact sites of the witness plates from experiments employing a 3mm projectile and 1mm thick target plates at velocities ranging from 1200 to 5500 m/s nominally.

These low-magnification images reinforce the findings from the optical imaging presented in section 3.1 for a 1mm target thickness, showing a distinct transition in crater morphology between impact velocities of 2403 and 4143 m/s.

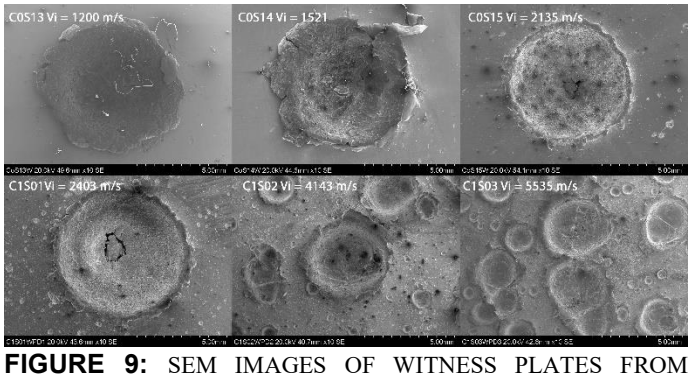


FIGURE 9: SEM IMAGES OF WITNESS PLATES FROM EXPERIMENTS INVOLVING A 1mm CFRP TARGET AND 3mm Al AT 10X MAGNIFICATION.

Figure 10 shows SEM images of what we believe are residual fibers from the CFRP panels in the same witness plates from Figure 9. These fibers are present across all impact velocities and vary in length from 10μm to 100 μm, while all

display a regular diameter of 5 μm, consistent with fibers from the targets, and provide evidence of fiber pullout and fiber fracture during the impact events.

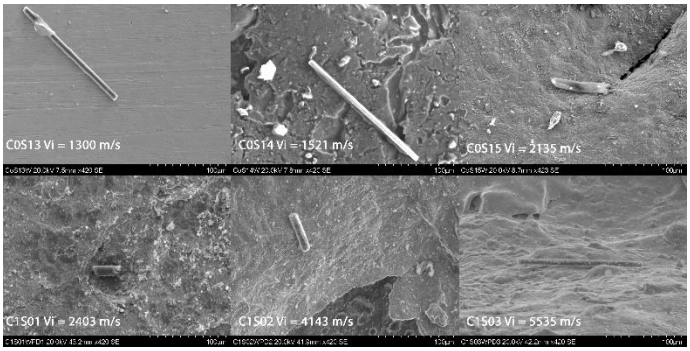


FIGURE 10: SEM IMAGES OF RESIDUAL FIBERS ON WITNESS PLATES FROM EXPERIMENTS INVOLVING A 1mm CFRP TARGET AND 3mm Al AT 420X MAGNIFICATION.

3.5 Results summary.

This work combines forensic approaches with in-situ measurements to provide a holistic approach for interrogating the underlying physical processes to better understand the impact phenomena associated with HVI in CFRP composites and attempts to isolate those effects related to strain rate.

In combination, the results from each of the analysis techniques employed indicate a distinct transition in the failure mechanics exhibited by the CFRP targets between the velocities of 2000 and 3000 m/s. This is evidenced by changes in witness plate debris patterns and projectile and debris cloud morphology between these velocities in the HSV footage. This is an interesting finding as the expected sound speed of the CFRP target lies within this range and implies that once the impact velocity exceeds the sound speed in the target, there is a distinct change in failure mechanics.

The results to date also indicate that there is a strain rate sensitivity present in the failure mechanics of the CFRP targets, where it may be possible to identify a threshold for changes in the behavior of the material by considering factors such as the sound speed and impact velocities in conjunction with strain rate thresholds during the event. The sound speed of the projectile material is also likely to play a critical role in the impact event; in this case, the expected sound speed of aluminum is around 5000 m/s. Further study of impacts in specific velocity ranges of 2000 to 3000 m/s and 5000 to 6500 m/s is planned to investigate strain rate effects in these regimes and investigate the relationships between sound speed in the target and projectile materials and the evolution of the failure modes presented.

4. CONCLUSION

In conclusion, our work has identified a clear evolution of failure modes and damage patterns presented during the HVI of commercially available QI CFRP composites of 1mm and 3mm thickness across the velocity range ca. 1-5.5 km/s when impacted by 3mm and 4mm diameter spherical 1000 series Al projectiles; this evolution is dependent on impact velocity and, consequently, strain rate, which follow from the strain rate-dependent relationships that emerge from the ballistic regime.

This study has also revealed dependency on projectile diameter and target thickness as a parameter influencing the failure modes of CFRP under HVI, as well as the complex interactions in the dissipation of impact energy across a variety of failure modes, including plastic deformation, delamination, fiber failure, thermomechanical coupling effects, and phase transitions, these varied failure mechanisms undergo a complex evolution as impact velocity and strain rates increase requiring further research to understand fully.

Further work investigating CFRP composition is proposed, and it intends to include aviation- and aerospace-grade CFRP composites and novel composites and sandwich panels. In tandem with adding a diverse set of target materials, an investigation into projectile parameters, including material, geometry, and impact angle, is planned.

These results will be important to several industries because they will provide a high-quality verification and validation dataset for numerical simulations and material models for CFRP composites and provide valuable insight into the underlying dynamic failure modes of this material class. This will enable engineers and designers to develop novel composite materials with superior HVI performance for structural, shielding, and armor applications across the defense, space, and aerospace sectors.

ACKNOWLEDGEMENTS

For the purposes of open access, the author has applied a Creative Commons Attribution (CC BY) license to any Accepted Author Manuscript version arising from this submission.

Data supporting this study will be available from Cranfield Online Research Data repository (CORD) at https://doi.org/10.17862/cranfield.rd.25731489 following an embargo until 01/08/2026.

This work was funded through an Engineering and Physical Sciences Council (EPSRC) Doctoral Training Partnership/studentship (20233/2023) to Cranfield University. We would like to thank the technical staff at Cranfield Defence and Security, in particular Mr Andrew Roberts, who assisted during the experimental campaigns. We would also like to acknowledge the support and contribution from the industrial partner, QinetiQ, through the DTP Partnership.

REFERENCES

[1] Andrew, J. J., Srinivasan, S. M., Arockiarajan, A. and Dhakal, H. N., “Parameters influencing the impact response of fiber-reinforced polymer matrix composite materials: A critical review,” Composite Structures **224**, 111007 (2019).

[2] Siviour, C. R. and Jordan, J. L., “High Strain Rate Mechanics of Polymers: A Review,” J. dynamic behavior mater. **2**(1), 15–32 (2016).

[3] Shui-sheng, Y., Yu-bin, L. and Yong, C., “The strain-rate effect of engineering materials and its unified model,” Lat. Am. j. solids struct. **10**(4), 833–844 (2013).

[4] Zhang, N., Qian, X., Zhang, Q., Zhou, G., Xuan, S., Wang, X. and Cai, D., “On strain rate effect and high-velocity impact behavior of carbon fiber reinforced laminated composites,” Thin-Walled Structures **194**, 111328 (2024).

[5] Gao, X., Zhang, M., Siddique, A., Yang, H., Liu, T. and Cao, M., “Damage evolution and failure mechanism of three-dimensional braided composite subjected to varied high strain-rate loadings,” Textile Research Journal **93**(7–8), 1783–1802 (2023).

[6] Ma, L., Liu, F., Liu, D. and Liu, Y., “Review of Strain Rate Effects of Fiber-Reinforced Polymer Composites,” Polymers **13**(17), 2839 (2021).

[7] Aoki, Y., Suemasu, H. and Ishikawa, T., “Damage propagation in CFRP laminates subjected to low velocity impact and static indentation,” Advanced Composite Materials **16**(1), 45–61 (2007).

[8] Bouvet, C. and Rivallant, S., “Damage tolerance of composite structures under low-velocity impact,” [Dynamic Deformation, Damage and Fracture in Composite Materials and Structures], Elsevier, 7–33 (2016).

[9] Cao, H., Ma, M., Jiang, M., Sun, L., Zhang, L., Jia, L., Tian, A. and Liang, J., “Experimental Investigation of Impactor Diameter Effect on Low-Velocity Impact Response of CFRP Laminates in a Drop-Weight Impact Event,” Materials **13**(18), 4131 (2020).

[10] Minak, G., Fotouhi, M. and Ahmadi, M., “Low-velocity impact on laminates,” [Dynamic Deformation, Damage and Fracture in Composite Materials and Structures], Elsevier, 147–165 (2016).

[11] Shi, Y., Pinna, C. and Soutis, C., “Low-velocity impact of composite laminates: Damage evolution,” [Dynamic Deformation, Damage and Fracture in Composite Materials and Structures], Elsevier, 89–119 (2023).

[12] Yashiro, S. and Ogi, K., “High-velocity impact damage in CFRP laminates,” [Dynamic Deformation, Damage and Fracture in Composite Materials and Structures], Elsevier, 169–191 (2016).

[13] Xu, M., Huang, G., Dong, Y. and Feng, S., “An experimental investigation into the high velocity penetration resistance of CFRP and CFRP/aluminium laminates,” Composite Structures **188**, 450–460 (2018).

[14] Xie, W., Zhang, W., Kuang, N., Li, D., Huang, W., Gao, Y., Ye, N., Guo, L. and Ren, P., “Experimental investigation of normal and oblique impacts on CFRPs by high velocity steel sphere,” Composites Part B: Engineering **99**, 483–493 (2016).

[15] Hazell, P. J. and Appleby-Thomas, G. J., “The impact of structural composite materials. Part 1: ballistic impact,” The Journal of Strain Analysis for Engineering Design **47**(7), 396–405 (2012).

[16] Appleby-Thomas, G. J., Wood, D. C., Hameed, A. and Leighs, J. A., “On the ballistic response of an aerospace-grade composite panel to non-spheroidised fragment simulants,” Composite Structures **119**, 90–98 (2015).

[17] Appleby-Thomas, G. J., Wood, D. C., Hameed, A., Painter, J., Le-Seelleur, V. and Fitzmaurice, B. C., “Investigation of the high-strain rate (shock and ballistic) response of the elastomeric tissue simulant Perma-Gel®,” International Journal of Impact Engineering **94**, 74–82 (2016).

[18] “Review of Thermoplastic Composites in AerospaceIndustry.”, IJETI **3**(1) (2022).

[19] Hazell, P. J., Stennett, C. and Cooper, G., “The effect of specimen thickness on the shock propagation along the in-fibre direction of an aerospace-grade CFRP laminate,” Composites Part A: Applied Science and Manufacturing **40**(2), 204–209 (2009).

[20] Giannaros, E., Kotzakolios, A., Kostopoulos, V. and Campoli, G., “Hypervelocity impact response of CFRP laminates using smoothed particle hydrodynamics method: Implementation and validation,” International Journal of Impact Engineering **123**, 56–69 (2019).

[21] Wicklein, M., Ryan, S., White, D. M. and Clegg, R. A., “Hypervelocity impact on CFRP: Testing, material modelling, and numerical simulation,” International Journal of Impact Engineering **35**(12), 1861–1869 (2008).

[22] He, Q.-G. and Chen, X., “Simulation method of debris cloud from fiber-reinforced composite shield under hypervelocity impact,” Acta Astronautica **204**, 402–417 (2023).

[23] Francesconi, A., Giacomuzzo, C., Kibe, S., Nagao, Y. and Higashide, M., “Effects of high-speed impacts on CFRP plates for space applications,” Advances in Space Research **50**(5), 539–548 (2012).

[24] “What are hypervelocity impacts?”, <https://www.esa.int/Enabling_Support/Operations/What_are_hypervelocity_impacts> (26 April 2024).

[25] “Carbon Fibre Sheet; 1mm, 2mm, 3mm - Easy Composites.”, <https://www.easycomposites.co.uk/high-strength-carbon-fibre-sheet> (26 April 2024).

[26] “EC-TDS-High-Strength-Carbon-Sheet.pdf.”, .

[27] “Phantom Cameras Vision Research Ltd.”, <https://www.phantomhighspeed.com/> (13 May 2024).

[28] Schindelin, J., Arganda-Carreras, I., Frise, E., Kaynig, V., Longair, M., Pietzsch, T., Preibisch, S., Rueden, C., Saalfeld, S., Schmid, B., Tinevez, J.-Y., White, D. J., Hartenstein, V., Eliceiri, K., Tomancak, P. and Cardona, A., “Fiji: an open-source platform for biological-image analysis,” Nat Methods **9**(7), 676–682 (2012).

[29] “PCC Software.”, <https://www.phantomhighspeed.com/resourcesandsupport/phantomresources/pccsoftware> (13 May 2024).



https://dspace.org/

Failure modes of CFRP panels under hypervelocity impact: the effects of strain rate between 1 km/s and 6 km /s

Lawrence, Jacob; Painter, Jonathan; Iordachescu, Alexandra; Footer, Charles J.; Seabright, Ryan M. ...

2024-09-09
ASME
https://doi.org/10.1115/HVIS2024-077
Lawrence J, Painter J, Iordachescu A, et al., (2024) Failure modes of CFRP panels under hypervelocity impact: the effects of strain rate between 1 km/s and 6 km/s. In: Proceedings of the 2024 17th Hypervelocity Impact Symposium, 8-13 September 2024, Tsukuba, Japan

Downloaded from a DSpace repository. https://dspace.org/